Appl. Phys. A (2014) 117:1259–1267
DOI 10.1007/s00339-014-8514-0

Applied Physics A
Materials Science & Processing

Dependence of the selectivity of SnO_2 nanorod gas sensors on functionalization materials

Sunghoon Park · Soohyun Kim · Hyunsung Ko · Chongmu Lee

Received: 4 March 2014 / Accepted: 12 May 2014 / Published online: 31 May 2014

Abstract Effects of functionalization materials on the selectivity of SnO_2 nanorod gas sensors were examined by comparing the responses of SnO_2 one-dimensional nanostructures functionalized with CuO and Pd to ethanol and H_2S gases. The response of pristine SnO_2 nanorods to 500 ppm ethanol was similar to 100 ppm H_2S. CuO-functionalized SnO_2 nanorods showed a slightly stronger response to 100 ppm H_2S than to 500 ppm ethanol. In contrast, Pd-functionalized SnO_2 nanorods showed a considerably stronger response to 500 ppm ethanol than to 100 ppm H_2S. In other words, the H_2S selectivity of SnO_2 nanorods over ethanol is enhanced by functionalization with CuO, whereas the ethanol selectivity of SnO_2 nanorods over H_2S is enhanced by functionalization with Pd. This result shows that the selectivity of SnO_2 nanorods depends strongly on the functionalization material. The ethanol and H_2S gas sensing mechanisms of CuO- and Pd-functionalized SnO_2 nanorods are also discussed.

1 Introduction

A range of CuO–SnO_2 composite nanostructures based on SnO_2 and CuO have been reported for H_2S sensing since the pioneering work of Moekawaetal [1] on CuO-doped SnO_2 thick films. These nanostructures include CuO–SnO_2 heterostructures [2–4], CuO-doped SnO_2 nanorods [5] and CuO-doped SnO_2 nanoribbons [6, 7]. The extraordinarily enhanced H_2S sensing properties of CuO-doped SnO_2 nanorods are usually explained by the formation of a resistive heterojunction between p-type CuO and n-type SnO_2 in an air atmosphere, the reaction of the semiconducting CuO with H_2S to form metallic CuS with a high conductivity upon exposure to H_2S, and the strong chemical affinity of the alkaline CuO toward the acidic H_2S gas [1, 7–9].

The response SnO_2 nanorods to NO_2 were reported to be degraded by functionalization with CuO [10], suggesting their selective sensing performance to H_2S. The selectivity of CuO-functionalized SnO_2 nanorods toward H_2S must be attributed to the above three mechanisms, but it might be related more intimately to the second one of the three mechanisms. This assumption is supported by the excellent sensing properties of Pd-functionalized CuO nanorods toward H_2S gas [11]. Nevertheless, the dependence of the selectivity of the SnO_2 nanorod-based gas sensors on the functionalization or doping material has not been clarified until now, even if there are many reports on the extraordinary H_2S sensing properties of CuO-functionalized SnO_2 nanorods. To elucidate the dependence of the selectivity on the functionalization or doping material, this study examined the effects of functionalization materials on the selectivity of SnO_2 nanorod gas sensors by comparing the responses of SnO_2 one-dimensional (1D) nanostructures functionalized with CuO and Pd to ethanol (C_2H_5OH) and H_2S gases. In addition, this study examined whether functionalization of SnO_2 nanostructures with CuO has adverse effects on the sensing properties of other gases than H_2S by examining the response of CuO-functionalized SnO_2 nanorods to ethanol gas.

S. Park · S. Kim · H. Ko · C. Lee (✉)
Department of Materials Science and Engineering, Inha University, 253 Yonghyun-dong, Nam-gu, Incheon 402-751, Republic of Korea
e-mail: cmlee@inha.ac.kr

2 Experimental

Figure 1 displays the process flow of sample preparation and sensing tests carried out in this study. CuO-functionalized SnO_2 nanorods were synthesized using a three-step process: the thermal evaporation of Sn powders in an oxidizing atmosphere, dipping in a $CuNO_3$ solution and thermal annealing. First, Au-coated Si was used as a substrate for the synthesis of 1D SnO_2 structures. A 3-nm-thick Au thin film was deposited on p-type (100) Si substrates by direct current (dc) magnetron sputtering. A quartz tube was mounted horizontally inside a tube furnace. A total of 99.99 % pure Sn powders were placed on the lower holder at the center of the quartz tube. The Au-coated Si substrate was placed on the upper holder, approximately 5 mm away from the Sn powders. The furnace was heated to 900 °C and maintained at that temperature for 1 h in a N_2/3 mol%-O_2 atmosphere with constant flow rates of O_2 (10 sccm) and N_2 (300 sccm). The total pressure was set to 1.0 Torr. Subsequently, the as-synthesized SnO_2 nanorods were dipped into a 1 M $Cu(NO_3)_2$ solution for 1 h and then cleaned with distilled water. The CuO-coated SnO_2 nanorods were annealed at 500 °C for 1 h in an oxygen atmosphere for 1 h (O_2 gas flow rate: 500 sccm).

The Pd-functionalized SnO_2 nanorods were also prepared by coating the as-synthesized SnO_2 nanorods with Pd using a wet chemistry method. An ethanolic palladium chloride solution (C_2H_5OH: $PdCl_2$ = 1,000:1) was prepared in a vial. The nanorod samples were immersed in that solution, and the vial was placed in a homemade ultraviolet (UV) box. The solution in a vial was then irradiated with 254 nm UV light at 3 mW/cm^2 for 20 min. Finally, the samples were annealed at 480 °C for 1 h in an Ar atmosphere. The Ar gas flow rate and process pressure were 100 cm^3/min and 1.0 Torr, respectively.

The morphology and structure of the products were characterized by scanning electron microscopy (SEM, Hitachi S-4200) operating at 10 kV and transmission electron microscopy (TEM, JEOL 2100F) with an accelerating voltage of 300 kV. The crystal structure of the nanorods was examined by glancing angle X-ray diffraction (XRD, Philips X'pert MRD diffractometer) using Cu K_α radiation (λ = 0.15406 nm) at a scan rate of 4°/min. The sample was arranged geometrically at a 0.5° glancing angle with a rotating detector.

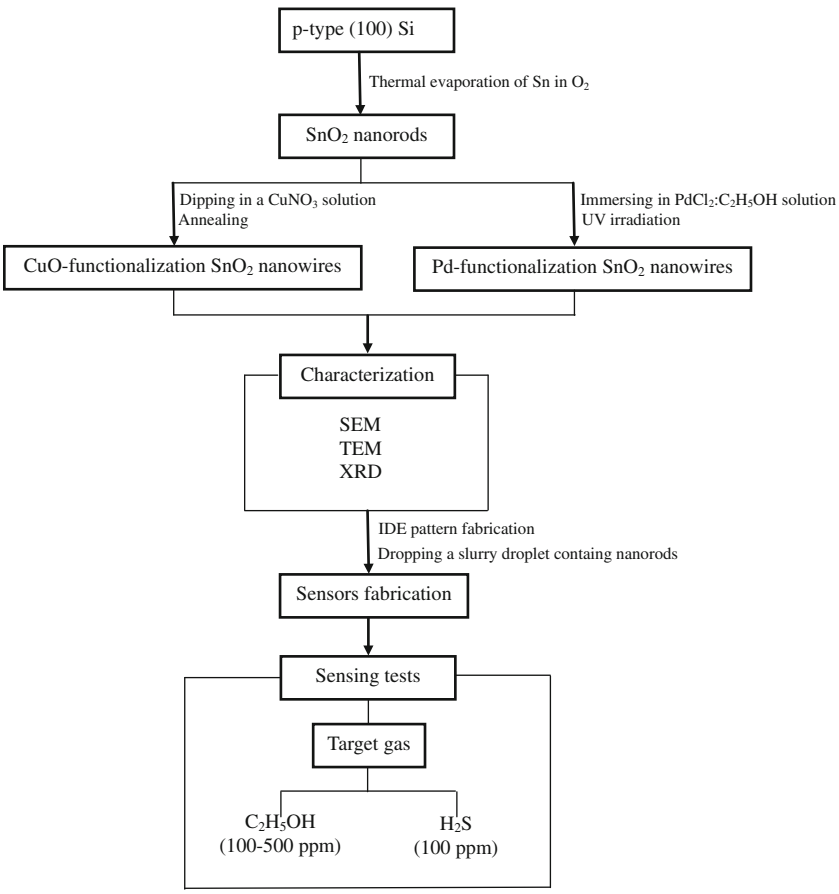

Fig. 1 Process flow of sample preparation and sensing tests

For the sensing measurements, Ni (~200 nm in thickness) and Au (~50 nm) thin films were deposited sequentially by sputtering to form electrodes using an interdigital electrode mask. Three different types of nanorod samples: pristine SnO_2 nanorods, CuO-functionalized SnO_2 nanorods and Pd-functionalized SnO_2 nanorods were dispersed ultrasonically in a mixture of deionized water (5 ml) and isopropyl alcohol (5 ml) and dried at 90 °C for 30 min. A 200-nm-thick SiO_2 film was grown thermally on single crystalline Si (100) substrates. A slurry droplet containing the nanorods (10 µl) was dropped onto the SiO_2-coated Si substrates equipped with a pair of interdigitated (IDE) Ni (~200 nm)/Au (~50 nm) electrodes with a gap of 20 µm. The gas sensing properties of the three different multiple networked nanorod sensors made from the three different types of nanorods were measured at 300 °C in a quartz tube placed in a sealed chamber with an electrical feed through. During the measurements, the sensors were placed in a sealed quartz tube with an electrical feed through. A set amount of C_2H_5OH (>99.99 %) or H_2S gas was injected into the testing tube through a microsyringe to obtain a C_2H_5OH concentration of 100–500 ppm or a H_2S concentrations of 100 ppm while the electrical current in the nanotubes was monitored. The response of the sensors is defined as $R_a/R_g \times 100(\%)$ both for C_2H_5OH and H_2S, where R_a and R_g are the electrical resistances in the sensors in air and the target gas, respectively.

3 Results and discussion

Figure 2a, b shows low-magnification and high-resolution TEM (HRTEM) images, respectively, of a typical CuO-functionalized SnO_2 nanorod. Figure 2c is selected area electron diffraction pattern corresponding to Fig. 2b. A comparison of Fig. 2a with the inset in Fig. 2a reveals that a CuO-functionalized SnO_2 nanorod (Fig. 2a) has many particles (dark globular particles) on the nanorod, whereas a pristine SnO_2 nanorod does not have such dark globular particles on it. HRTEM image (Fig. 2b) revealed fringes with spacings of 0.264 and 0.237 nm, corresponding to the interplanar distances of the {101} and {200} lattice planes, respectively, in bulk crystalline SnO_2. Figure 2c shows dim diffractions spots assigned to monoclinic-structured CuO particles as well as intense diffraction spots assigned to tetragonal-structured SnO_2 nanorods, verifying the existence of CuO particles on the surface of SnO_2 nanorods. The XRD pattern of CuO-functionalized SnO_2 nanorods (Fig. 2d) showed both the reflection peaks assigned to tetragonal-structured SnO_2 with lattice constants of $a = 0.4737$ nm and $c = 0.3186$ nm (JCPDS No. 88-0287) and those assigned to monoclinic CuO with lattice constants of $a = 0.4689$ nm, $b = 0.342$ nm, $c = 0.513$ nm, $\beta = 99.57°$(JCPDS No. 89-5899).

Figure 3a shows the low-magnification TEM image of a typical Pd-functionalized SnO_2 nanorod. Many small particles with diameters ranging from 3 to 20 nm are observable on the surface of the nanorod. An HRTEM image shows the two different regions with different fringe patterns clearly: (a) the upper part of the image shows a fringe pattern with a spacing of 0.225 corresponding to the interplanar distance of the {111} lattice plane in bulk crystalline Pd, whereas (b) the lower part shows two types of fringes with spacings of 0.264 and 0.237 nm, corresponding to the interplanar distances of the {101} and {200} lattice planes, respectively, in bulk crystalline SnO_2, respectively. The corresponding diffraction pattern (Fig. 3c) displays dim spots as well as intense diffraction spots assigned to tetragonal-structured SnO_2. A structural analysis of the dim spotty pattern identified the pattern to be of face-centered cubic Pd, whereas small peaks located at ~39°, ~47° and ~69° were assigned to the (111), (200) and (220) reflections, respectively, of face-centered cubic-structured Pd. The XRD pattern of Pd-functionalized SnO_2 nanorods (Fig. 3d) shows several small reflection peaks assigned to Pd as well as tall reflection peaks assigned to SnO_2. The relatively weak reflection intensities of Pd compared to those of SnO_2 might be due to the far smaller amount of Pd compared to that of SnO_2 in the nanorods.

Figure 4a–c shows the dynamic responses of the pristine, CuO-functionalized SnO_2 nanorods and Pd-functionalized SnO_2 nanorods to a reducing gas C_2H_5OH at 300 °C, respectively. The sensor responded well to ethanol gas. The resistance decreased rapidly when the nanorod sensors were exposed to ethanol gas and recovered almost to the initial value when the ethanol gas supply was stopped and air was introduced. The responses of the CuO-functionalized SnO_2 nanorods were quite stable and reproducible for repeated testing. Table 1 lists the responses calculated from Fig. 4a–c. The pristine SnO_2 nanorods showed responses of approximately 137, 151, 165, 181 and 211 % to 100, 200, 300, 400 and 500 ppm C_2H_5OH, respectively. In contrast, the CuO-functionalized SnO_2 nanorods and Pd-functionalized SnO_2 nanorods showed corresponding responses of approximately 170, 192, 240, 320 and 696 % and 173, 195, 250, 365 and 590 %, respectively, to 100, 200, 300, 400 and 500 ppm C_2H_5OH. Consequently, functionalizing SnO_2 nanorods with CuO and Pd led to 1.2–3.3- and 1.3–2.8-fold stronger responses, respectively, to 100–500 ppm ethanol gases.

Figure 4d shows the responses determined from Fig. 4a–c as a function of the C_2H_5OH concentration. A linear relationship was observed between the response and the ethanol concentration in the ethanol gas concentration

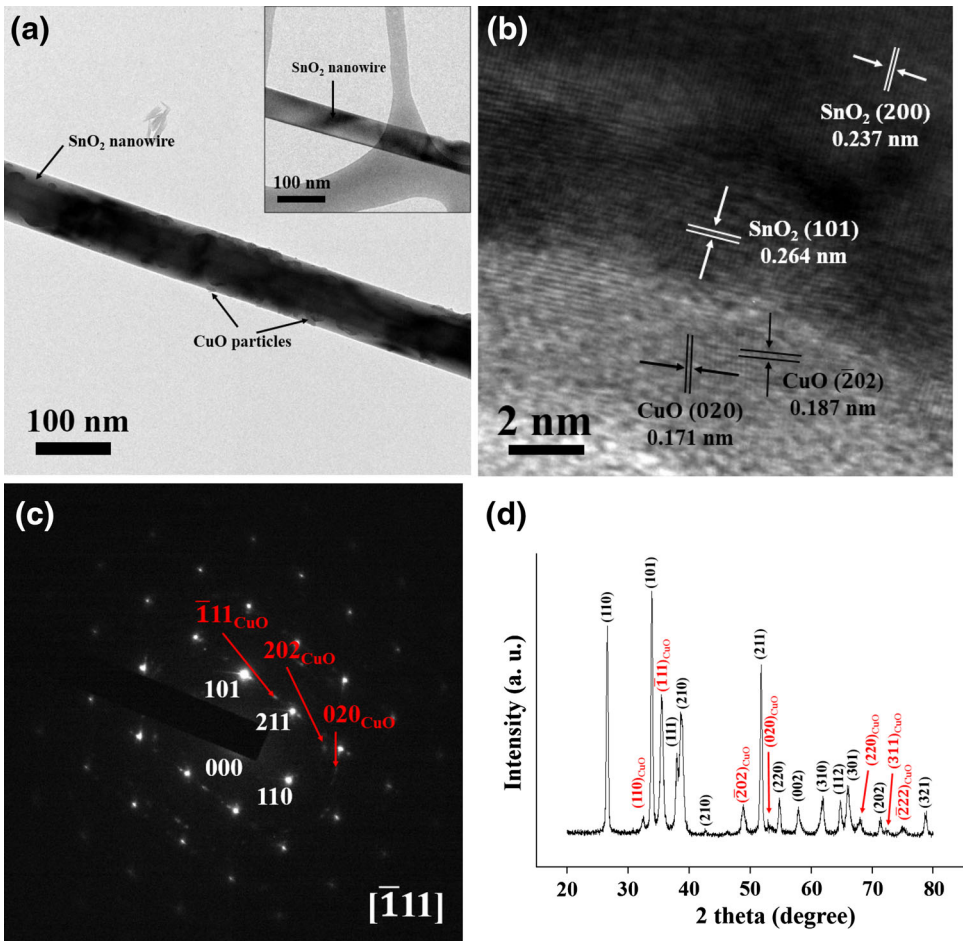

Fig. 2 **a** Low-magnification TEM image of a typical CuO-functionalized SnO_2 nanorod. **b** High-resolution TEM image and **c** corresponding SAED pattern of the CuO-SnO_2 interface region of a typical CuO-functionalized SnO_2 nanorod. **d** XRD patterns of the CuO-functionalized SnO_2 nanorods

range of 100–500 ppm. The response of an oxide semiconductor can normally be expressed as $R = A\ [C]^n + B$, where A and B, n, and [C] are constants, exponent, and target gas concentration, respectively [12]. Data fitting gave $R = 1.18\ [C] - 29.9$, $R = 1.00\ [C] + 13.5$ and $R = 0.179\ [C] + 115.2$ for the CuO-functionalized SnO_2 nanorods, Pd-functionalized SnO_2 nanorods and pristine SnO_2 nanorods, respectively. The responses of these three different SnO_2 nanorod sensors tended to increase with increasing C_2H_5OH gas concentration, but the responses of the CuO- or Pd-functionalized SnO_2 nanorods tended to increase more rapidly than that of the pristine SnO_2 nanorods. In particular, the response of the CuO-functionalized SnO_2 nanorods was higher than Pd-functionalized SnO_2 nanorods at high C_2H_5OH concentrations, whereas the former was lower than the latter at low C_2H_5OH concentrations.

Another thing to note is the jump in response between 400 and 500 ppm C_2H_5OH. It is not well understood at present why the sensing response to 500 ppm ethanol was significantly increased compared to the ones of 400 ppm ethanol for the functionalized SnO_2 nanorods. In general, the sensitivity or response can jump at a critical temperature as the temperature increases because of change in sensing mechanism. On the other hand, it is seldom that the sensitivity or response jumps at a critical gas concentration as the concentration increase because of no change in sensing mechanism. A further systematic study may be necessary to reveal the cause of the significant increase. The significant increase in response in this study is probably due to the experimental error rather than due to change in sensing mechanism. The important concentration range in detecting gas depends on the kind of gas. For example, in the case of ethanol sensing, the gas concentrations studied commonly range from 100 to 10,000 ppm. Most previous studies reported that the sensing response increased quite a bit in the ethanol concentration range from 400 to 500 ppm with increasing the ethanol concentration. Therefore, the result in this study that the significant increase in the sensing response to 500 ppm ethanol was significantly increased compared to the ones of 400 ppm ethanol is not much surprising. We imagine further increases in ethanol concentration to 10,000 ppm might lead to the saturation of the ethanol sensing properties.

Figure 5 compares the responses of the pristine, CuO-functionalized and Pd-functionalized SnO_2 nanorods to

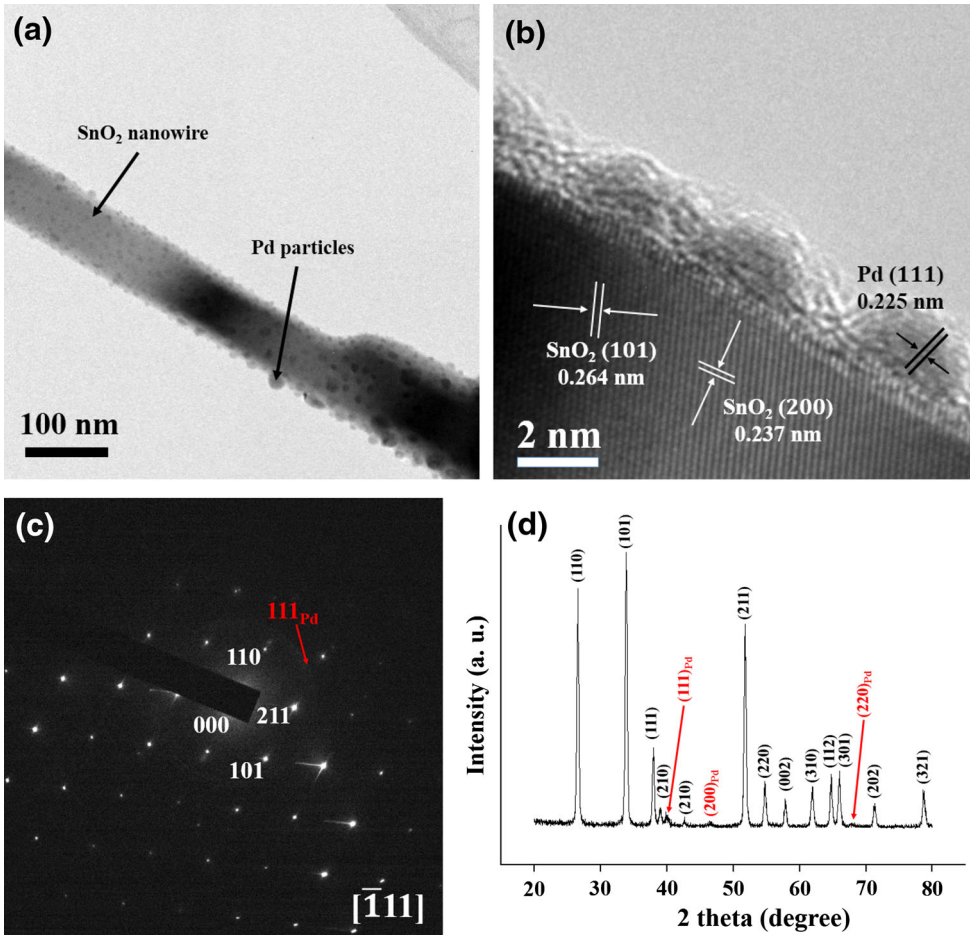

Fig. 3 **a** Low-magnification TEM image of a typical Pd-functionalized SnO_2 nanorod. **b** High-magnification TEM image and **c** corresponding SAED pattern of the Pd-SnO_2 interface region of a typical Pd-functionalized SnO_2 nanorod. **d** XRD pattern of Pd-functionalized SnO_2 nanorods

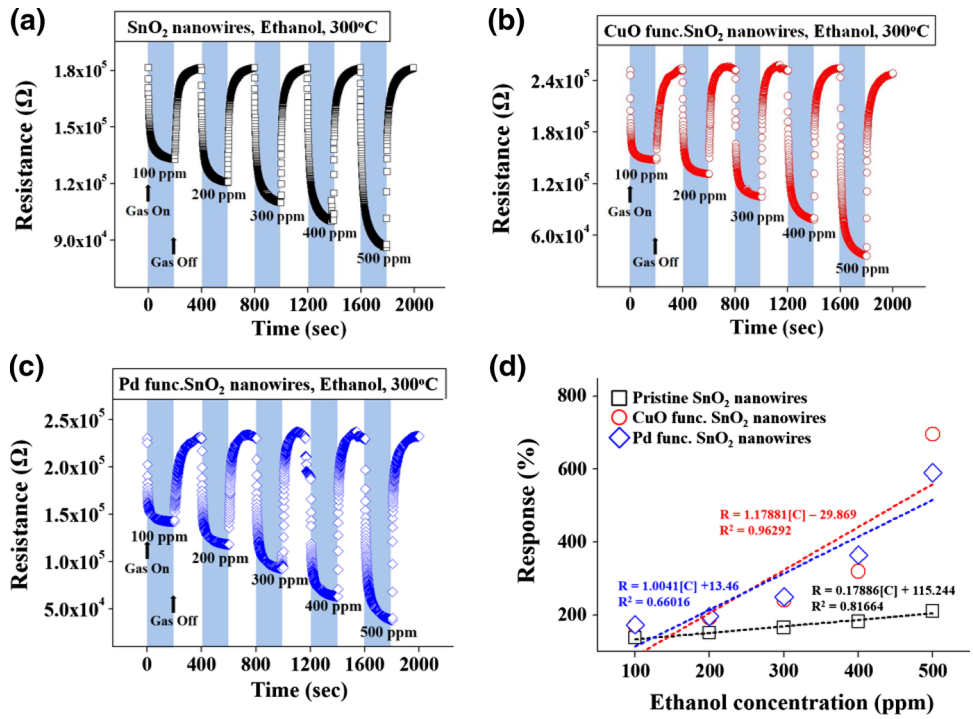

Fig. 4 Electrical responses of the gas sensors fabricated from **a** pristine, **b** CuO-functionalized SnO_2 nanorods and **c** Pd-functionalized SnO_2 nanorods to 100, 200, 300, 400 and 500 ppm ethanol gas at 300 °C. **d** Responses of pristine, CuO-functionalized and Pd-functionalized SnO_2 nanorods as a function of ethanol concentration

Table 1 Responses of the pristine, CuO-functionalized and Pd-functionalized SnO_2 nanorods to ethanol gas

Ethanol conc. (ppm)	Response (%)		
	SnO_2	CuO-functionalized SnO_2	Pd-functionalized SnO_2
100	136.67	170.64	172.64
200	150.62	191.97	195.84
300	165.07	240.40	249.87
400	181.48	319.66	364.94
500	210.67	696.20	590.15

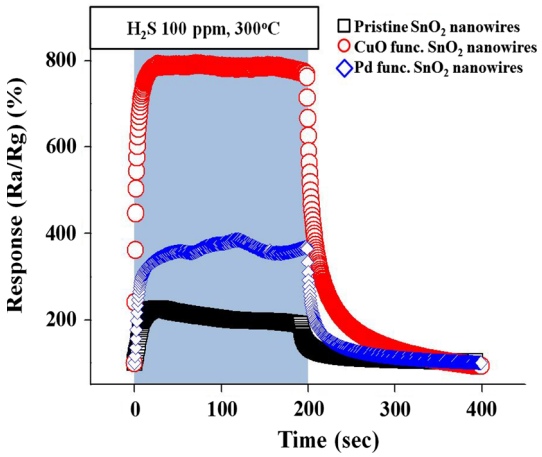

Fig. 5 Comparison of the responses of pristine, CuO-functionalized and Pd-functionalized SnO_2 nanorods to H_2S gas

Table 2 Responses of pristine, CuO-functionalized and Pd-functionalized SnO_2 nanorods to 100 ppm H_2S gas and 500 ppm ethanol

Nanomaterials	Response to 100 ppm H_2S gas (%)	Response to 500 ppm C_2H_5OH (%)
Pristine SnO_2 nanorods	207.66	210.67
CuO-functionalized SnO_2 nanorods	798.12	696.20
Pd-functionalized SnO_2 nanorods	387.54	590.15

H_2S gas. As reported previously, CuO-functionalized SnO_2 nanorods showed considerably stronger responses than those of the Pd-functionalized and pristine SnO_2 nanorods, suggesting that the CuO-functionalized SnO_2 nanorods are an excellent H_2S gas sensor. Table 2 showed the difference in selectivity between the CuO- and Pd-functionalized SnO_2 nanorods. The selectivity of the two nanomaterials can be compared reasonably from the responses summarized in Table 2 because the pristine SnO_2 nanorods showed similar response to 100 ppm H_2S to that to 500 ppm C_2H_5OH. CuO-functionalized SnO_2 showed a stronger response to 500 ppm ethanol than to 100 ppm H_2S, but the difference was small. In contrast, the Pd-functionalized SnO_2 nanorods showed a considerably stronger response to100 ppm H_2S than that to 500 ppm C_2H_5OH. Therefore, the ethanol selectivity of the SnO_2 nanorods over H_2S is enhanced by functionalization with Pd, whereas the H_2S selectivity of SnO_2 nanorods over C_2H_5OH is enhanced by functionalization with CuO.

Figure 6a–c shows the dependence of the responses of CuO-functionalized and Pd-functionalized SnO_2 nanorods to ethanol gas. Both the CuO-functionalized (Fig. 6a) and Pd-functionalized (Fig. 6b) SnO_2 nanorods show that their responses to 500 ppm ethanol increased with increasing temperature up to 300 °C and then decreased with a further increase in temperature from 300 to 350 °C. The response of CuO-functionalized SnO_2 nanorods was higher than that of Pd-functionalized SnO_2 nanorods at any temperature in the temperature range of 200–350 °C (Fig. 6c). These results suggest that the relative selectivities of the SnO_2 nanorods functionalized with two different materials do not change with temperature in this temperature range. In other words, the relative sensitivities and selectivities of the SnO_2 nanorods are independent of the temperature and functionalization material.

The ethanol gas sensing mechanism of the SnO_2 nanorod sensor can be modeled using the surface-depletion model [13]. When the SnO_2 nanorod sensor is exposed to air, it interacts with oxygen by transferring electrons from the conduction band to the adsorbed oxygen atoms, forming ionic species, such as O^-, O^{2-} and O_2^-, as illustrated below.

$$O_2(g) \rightarrow O_2(ads) \quad (1)$$

$$O_2(ads) + e^- \rightarrow O_2^-(ads) \quad (2)$$

$$O_2^-(ads) + e^- \rightarrow 2O^-(ads) \quad (3)$$

$$O^-(ads) + e^- \rightarrow O^{2-}(ads) \quad (4)$$

A depletion region is created in the wall of the SnO_2 nanorods due to the consumption of electrons in the surface region of the SnO_2 nanorods [14], resulting in an increase in the electrical resistance of the SnO_2 nanorods. The surface depletion layer thickness, the potential barrier and the electrical resistance increase with increasing the number of oxygen ions on the surface [15].

When the sensor is exposed to ethanol gas, C_2H_5OH molecules will react with the preexisting oxygen ions on the SnO_2 nanorod surface to form CO_2 and H_2O according to the following equation and the electrons are released back to the SnO_2 nanorods [16]:

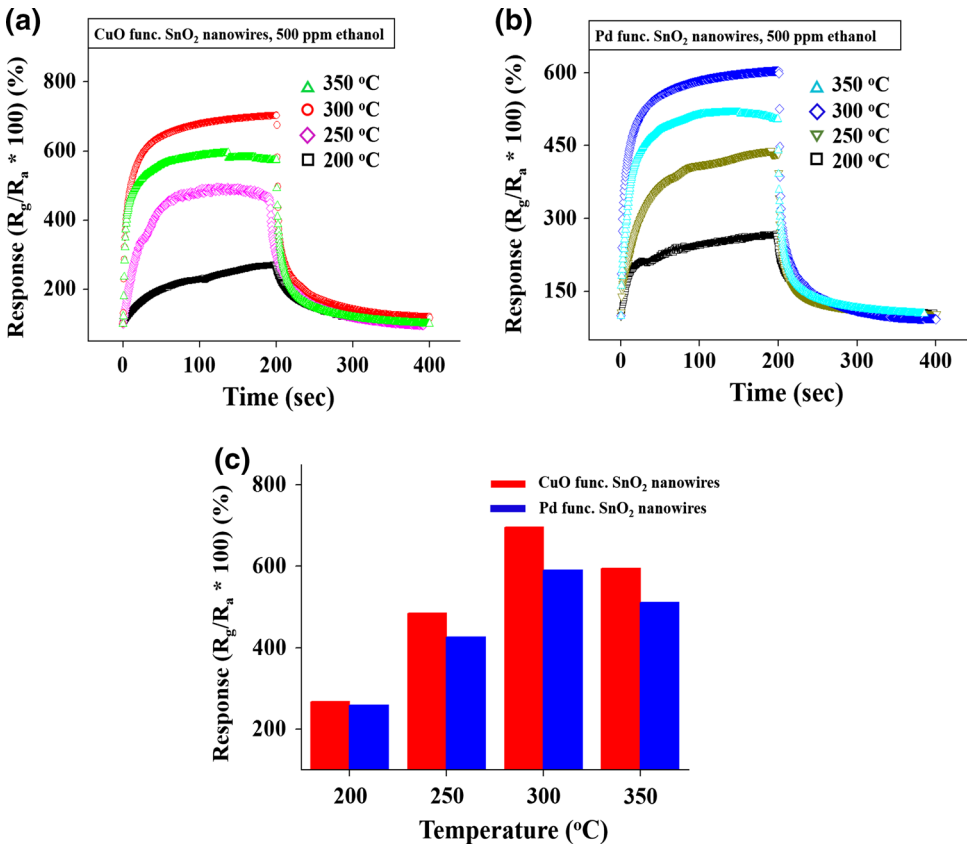

Fig. 6 Responses of **a** CuO-functionalized and **b** Pd-functionalized SnO_2 nanorods to 500 ppm ethanol gas for different temperatures. **c** Comparison of the responses of CuO-functionalized and Pd-functionalized SnO_2 nanorods to 500 ppm ethanol gas at different temperatures in the temperature range of 200–350 °C

$$CH_3CH_2OH\ (gas) \rightarrow CH_3CH_2OH\ (ads) \quad (5)$$

$$CH_3CH_2OH\ (ads) + 6O^-(ads) \rightarrow 2CO_2(gas) + 3H_2O\ (gas) + 6e^- \quad (6)$$

This leads to an increase in carrier concentration in the SnO_2 nanorod surface and a decrease in the surface depletion layer width. In other words, the depleted electrons are returned to the conduction band, which results in a sharp decrease in the electrical resistance of the SnO_2 nanorod sensors.

The enhanced response of the CuO-functionalized SnO_2 nanorods to ethanol gas might be due to the formation of a p-CuO–n-SnO_2 junction. The modulation of electron transport by this pn-junction with an adjustable energy barrier height would result in response to C_2H_5OH as high as that of the Pd-functionalized SnO_2 nanorods. In contrast, the main underlying sensing mechanism of the p-CuO (nanoparticle)/n-SnO_2 (nanorod) heterostructures upon exposure to H_2S was described in the literature [17]. The chemically specific transformation from p-CuO to metallic CuS modifies the depleted region formed at the p-CuO/n-SnO_2 interface and restricts the conduction channel inside the nanorods in an oxygen-rich atmosphere. Upon exposure to H_2S, copper oxide undergoes a sulphurization process to form CuS with metallic characteristics according to the following reaction [18–21]:

$$CuO + H_2S \rightarrow CuS + H_2O \quad (7)$$

$$CuS + (3/2)\ O_2 \rightarrow CuO + SO_2 \quad (8)$$

Under these conditions, highly resistive p-CuO transforms to conducting Cu_2S, changing the heterostructure from a standard pn-junction to a metal–semiconductor junction. The breakup of the pn-junction and the formation of a metal–semiconductor junction increase the conduction section in the nanorod, leading to a significant improvement in conductivity. Second-order effects such as the oxidation of CuS by oxygen adsorbed on the CuO nanoparticles might also contribute to p–n junction modulation. These two phenomena lead to much stronger response to H_2S gas than that caused by standard redox surface reactions in metal oxides [22].

On the other hand, the enhanced responses of the Pd-functionalized SnO_2 nanorods to C_2H_5OH and H_2S gases can be explained by the combination of a catalytic mechanism based on the spillover effect and an electronic mechanism [23]. In particular, the selectivity of the Pd-functionalized SnO_2 nanorods to C_2H_5OH over H_2S gases can be explained by the catalytic activity of C_2H_5OH

oxidation boosted by Pd. Many oxide semiconductors including SnO_2 commonly show selective detection to C_2H_5OH. This high C_2H_5OH selectivity was reported to be due to the high oxygen concentration and high catalytic oxidation activity of C_2H_5OH [23]. Actually, the adsorbed C_2H_5OH molecules on the Pd surface would react with adsorbed oxygen species on the SnO_2 surface, and hence, the sensitivity of the metal oxide sensor should depend upon the catalytic activity for C_2H_5OH oxidation. Therefore, the high C_2H_5OH selectivity of the Pd-functionalized SnO_2 nanorod sensor at 300 °C over H_2S might also be attributed to the higher oxygen concentration and the higher catalytic oxidation activity of C_2H_5OH on Pd surface than that of H_2S. One thing worthy of noting regarding the gas sensing selectivity of the Pd-functionalized SnO_2 nanorods is that the roles of Pd in the gas sensing reaction, as reported in the literature, have not always been consistent [23]. This suggests that Pd plays a complicated role that varies according to its doping concentration [24, 25], sensor temperature [26], loading methods [24, 27], and the species of target gas [28–31].

4 Summary

Multiple networked CuO- and Pd-functionalized SnO_2 nanorod sensors showed significantly stronger electrical responses to C_2H_5OH and H_2S gases at 300 °C compared to their pristine SnO_2 nanorod counterparts. The pristine SnO_2 nanorod sensors exhibited a response of 211 % to 500 ppm C_2H_5OH at 300 °C, whereas the CuO- and Pd-functionalized SnO_2 nanorod sensors showed a response of 696 and 590 %, respectively, under the same conditions. On the other hand, the pristine SnO_2 nanorod sensors exhibited a response of 208 % to 100 ppm C_2H_5OH at 300 °C, whereas the CuO- and Pd-functionalized SnO_2 nanorod sensors showed a response of 798 % and 388 %, respectively, under the same conditions. The C_2H_5OH selectivity of the SnO_2 nanorods over H_2S was enhanced by functionalization with Pd, whereas the H_2S selectivity of the SnO_2 nanorods over C_2H_5OH was enhanced by functionalization with CuO. The enhanced responses of the CuO-functionalized SnO_2 nanorods to ethanol and H_2S gases can be attributed to the formation of a p-CuO–n-SnO_2 junction and a metal–semiconductor junction, respectively. Both the CuO- and Pd-functionalized SnO_2 nanorods showed that their responses to 500 ppm ethanol increased with increasing temperature up to 300 °C and then decreased with a further increase in temperature from 300 to 350 °C. On the other hand, the relative selectivities of the SnO_2 nanorods functionalized with two different materials do not change with temperature in the temperature range of 200–350 °C. The enhanced responses of the Pd-functionalized SnO_2 nanorods to C_2H_5OH and H_2S gases can be explained by the combination of a catalytic mechanism based on the spillover effect and an electronic mechanism. In particular, the selectivity of the Pd-functionalized SnO_2 nanorods to C_2H_5OH over H_2S gases can be explained by the catalytic activity of C_2H_5OH oxidation boosted by Pd.

Acknowledgments This research was supported by Basic Science Research Program through the National Research Foundation of Korea (NRF) funded by the Ministry of Education (2010-0020163).

References

1. J. Tamaki, T. Maekawa, N. Miura, N. Yamazoe, Sens. Actuators B **9**, 197–203 (1992)
2. J.H. Yoon, J.S. Kim, Met. Mater. Int. **00**, 773–777 (2010)
3. L. He, Y. Jia, F. Meng, M. Li, J. Liu, J. Mater. Sci. **44**, 4326–4333 (2009)
4. A. Khanna, R. Kumar, S.S. Bhatti, Appl. Phys. Lett. **82**, 4388–4390 (2003)
5. X. Xue, L. Xing, Y. Chen, S. Shi, Y. Wang, T. Wang, J. Phys. Chem. **C112**, 12157–12160 (2008)
6. F.N. Meng, X.P. Di, H.W. Dong, Y. Zhang, Sens. Actuators B **182**, 197–204 (2013)
7. A. Chowdhri, P. Sharma, V. Gupta, K. Sreenivas, K.V. Rao, J. Appl. Phys. **92**, 2172–2179 (2002)
8. G. Sarala, S. Manorama, V.J. Rao, High sensitivity and selectivity of an SnO_2 sensor to H2S at around 100 · C. Sens. Actuators B **28**, 31–37 (1995)
9. I.S. Hwang, J.K. Choi, S.J. Kim, K.Y. Dong, J.H. Kwon, B.K. Ju, J.H. Lee, Enhanced H_2S sensing characteristics of SnO2 nanowires functionalized with CuO. Sens. Actuators B **142**, 105–110 (2009)
10. S. Kim, H. Na, S. Choi, D. Kwak, H. Kim, Novel growth of CuO-functionalized, branched SnO_2 nanowires and their application to H_2S sensors. J. Phys. D Appl. Phys. **45**, 205301–205308 (2012)
11. H. Kim, C. Jin, S. Park, S. Kim, C. Lee, H_2S gas sensing properties of bare and Pd-functionalized CuO nanorods. Sens. Actuators B **161**, 594–599 (2012)
12. D.E. Williams, *Solid State Gas Sensors* (Hilger, Bristol, 1987)
13. O. Safonova, G. Delabouglise, B. Chenevier, A. Gaskov, M. Labeau, CO and NO_2 gas sensitivity of nanocrystalline tin dioxide thin films doped with Pd, Ru and Rh. Mater. Sci. Eng. C **21**, 105–111 (2002)
14. A. Kolmakov, M. Moskovits, Chemical sensing and catalysis by one-dimensional metal-oxide nanostructures. Annu. Rev. Mater. Res. **34**, 151–180 (2004)
15. S. Morrison, Selectivity in semiconductor gas sensors. Sens. Actuators B **12**, 425–440 (1987)
16. J. Li, H. Fan, X. Jia, W. Yang, P. Fang, Enhanced blue-green emission and ethanol sensing of Co-doped ZnO nanocrystals prepared by a solvothermal route. Appl. Phys. A **98**, 537–542 (2010)
17. J. Tamaki, K. Shimanoe, Y. Yamada, Y. Yamamoto, N. Miura, N. Yamazoe, Dilute hydrogen sulfide sensing properties of CuO–SnO_2 thin film prepared by low-pressure evaporation method. Sens. Actuators, B **49**, 121–125 (1998)
18. T. Pagnier, M. Boulova, A. Galerie, A. Gaskov, G. Lucazeau, Reactivity of SnO2–CuO nanocrystalline materials with H_2S: a coupled electrical and Raman spectroscopic study. Sens. Actuators B Chem. **71**, 134–139 (2000)

19. J. Dunn, C. Muzenda, Thermal oxidation of covellite (CuS). Thermochim. Acta **369**, 117–123 (2001)
20. S. Wang, Q. Huang, X. Wen, X. Li, S. Yang, Thermal oxidation of Cu_2S nanowires: a template method for the fabrication of mesoscopic CuO (x = 1, 2) wires. Phys. Chem. Chem. Phys. **4**, 3425–3429 (2002)
21. C. Mu, J. He, Confined conversion of CuS nanowires to CuO nanotubes by annealing-induced diffusion in nanochannels. Nanoscale Res. Lett. **6**, 150–155 (2011)
22. N. Barsan, U. Weimar, Conduction model of metal oxide gas sensors. J. Electroceram. **7**, 143–167 (2001)
23. J.K. Choi, I.S. Hwang, S.J. Kim, J.S. Park, S.S. Park, U. Jeong, Y.C. Kang, J.H. Lee, Design of selective gas sensors using electrospun Pd-doped SnO_2 hollow nanofibers. Sens. Actuators B **150**, 191–199 (2010)
24. S. Matsushima, T. Maekawa, J. Tamaki, N. Miura, N. Yamazoe, New methods for supporting palladium on a tin oxide gas sensor. Sens. Actuators B **9**, 71–78 (1992)
25. M. Yuasa, T. Masaki, T. Kida, K. Shimanoe, N. Yamazoe, Nano-sized PdO loaded SnO_2 nanoparticles by reverse micelle method for highly sensitive CO gas sensor. Sens. Actuators B **136**, 99–104 (2009)
26. L. Liu, T. Zhang, S. Li, L. Wang, T. Tian, Preparation, characterization, and gas-sensing properties of Pd-doped In_2O_3 nanofibers. Mater. Lett. **63**, 1975–1977 (2009)
27. C.-B. Lim, S. Oh, Microstructure evolution and gas sensitivities of Pd-doped SnO_2-based sensor prepared by three different catalyst-addition process. Sens. Actuators B **30**, 223–231 (1996)
28. N. Yamazoe, K. Kurokawa, T. Seiyama, Effects of additives on semiconductor gas sensor. Sens. Actuators **4**, 283–289 (1983)
29. G. Tournier, C. Pijolat, R. Lalauze, B. Patissier, Selective detection of CO and CH_4 with gas sensors using SnO_2 doped with palladium. Sens. Actuators B **26–27**, 24–28 (1995)
30. Y.C. Lee, H. Huang, O.K. Tan, M.S. Tse, Semiconductor gas sensor based on Pd doped SnO_2 nanorod thin films. Sens. Actuators B **132**, 239–242 (2008)
31. Y. Zhang, Q. Xiang, J. Xu, P. Xu, Q. Pan, F. Li, Self-assemblies of Pd nanoparticles on the surfaces of single crystal ZnO nanowires for chemical sensors with enhanced performances. J. Mater. Chem. **19**, 4701–4706 (2009)